HST AR Proposal

Modeling the Time-Dependent Structure of M31's Dark Matter Halo in the Presence of its Massive Satellite M33

M31 and its satellites are emerging as one of the most exciting new testbeds of galaxy dynamics and cold dark matter (CDM) theory. Due to its proximity, M31 is the only galaxy other than the Milky Way for which we can reconstruct the orbits of its satellites and infer its assembly history. Ongoing *HST* observations are revealing the 3-D velocities of M31 and its satellites for the first time, laying the groundwork for determining the dynamical history of the system. However, orbit reconstruction also requires an accurate model of M31's DM distribution, and current models are too simplistic. State-of-the-art models assume a static, adiabatically contracted NFW profile and neglect the perturbations induced by M31's most massive satellite, M33. We propose to create a suite of high-resolution *N*-body simulations of the interaction between M31 and M33 that will map the time-dependent structure of M31's DM halo in the presence of M33 for the first time. *HST* has already been used to measure proper motions in the M31 system, creating archival datasets that cannot be interpreted without accounting for M33's influence. Our simulations will provide a cutting-edge model of the M31/M33 gravitational potential that will be crucial for accurately inferring M31's assembly history from existing and future *HST* measurements. This program will provide the foundation for the first detailed dynamical picture of a galactic ecosystem other than the Milky Way, opening a new frontier for testing galaxy formation theories in the CDM paradigm and studying the nature of DM itself.

- **Scientific Justification**

1. M31's Assembly History is a Powerful Near-Field Cosmology Probe

Reconstructing the orbits of satellite galaxies provides crucial probes of Lambda-Cold Dark Matter (ΛCDM) structure formation. The orbits of satellite galaxies and other halo tracers: 1) map the gravitational potential and DM distribution of the host galaxy (e.g. Price-Whelan+2014, Bonaca & Hogg 2018, Bonaca+2019); 2) reveal kinematic associations such as groups and planes of dwarf galaxies, testing hierarchical growth on smaller scales (e.g. Pawlowski+2012, Ibata+2013, Patel+2020); and 3) can be used to infer the host galaxy's assembly history (e.g. Carlberg 2017, Kruijssen+2019, Naidu+2021). M31 and its system of satellites is the only other galaxy system (besides our own Galaxy) that is close enough for modern facilities to measure proper motions (PMs) with sufficient accuracy ($\lesssim 10$ km/s) to meaningfully reconstruct orbits (Patel+2020). Despite this, M31 remains relatively under-studied compared to the Milky Way (MW), making M31 the next frontier for orbit reconstruction.

In the era of precision astrometry, measurements of M31 and a growing number of its bright satellites have already revolutionized our understanding of the dynamics of the system. For example, water-maser and *HST* PMs of M31 and its most massive satellite, M33, indicate that M33 is likely recently captured by M31 (Brunthaler+2005; Sohn+2012; Patel+2017a, hereafter P17; Patel+2017b). This result lies in contrast to earlier works which proposed a recent pericenter passage of M33 to explain the warp in its gas disk (McConnachie+2009, Putman+2009). *Gaia* PMs of M31 have suggested M31 is not moving as directly toward the MW as previously thought (van der Marel+2019). *HST* PMs of NGC 147 and NGC 185 have strengthened the evidence for the Great Plane of Andromeda (GPoA), in which a collection of M31's satellites orbit in a coherent plane (Sohn+2020). As ongoing *HST* observations (GO-15902, PI Weisz) seek to ensure *all* of M31's 27 known satellites (as of 2013; Ibata+2013) have measured PMs, the stage is set for reconstructing the assembly history of our nearest galactic neighbor.

However, orbit reconstruction also requires a model of the dark matter (DM) distribution and resulting gravitational potential of the system (e.g. Bonaca+2014, Gómez+2015). There are no such models for M31 that account for its massive satellite, M33, which contributes $\sim 2 \times 10^{11} M_\odot$ of DM to the system (~ 10% of M31's own mass; P17 and references therein). As such, it is expected to significantly perturb M31's DM (Garavito-Camargo+2021b). *No current models of M31's DM distribution include the distortions induced by M33, making accurate orbit reconstruction of M31's satellites with these models impossible.*

<u>We propose to create a suite of high-resolution (m~$10^4\,M_\odot$) *N*-body simulations of the M31/M33 interaction.</u> These simulations will be combined with a basis function expansion (BFE) technique to extract analytic descriptions of the DM density field and gravitational potential, providing the first-ever models of the combined M31/M33 halo and potential as a function of time. The proposed models will provide the necessary framework for using *HST* datasets to reconstruct M31's assembly history, enabling new tests of the physics of galaxy assembly and the interplay between galaxies and DM.

2. M33 Significantly Perturbs M31's Dark Matter Distribution

The state-of-the-art in modeling the combined M31+M33 DM distribution is to treat the two galaxies as separate, spherically symmetric DM halos. These halos are allowed to change position, but not shape, in response to each other's gravity (P17). However, high-resolution *N*-body simulations of the MW/LMC system by Garavito-Camargo+(2019, hereafter G19) have demonstrated that massive satellites induce significant perturbations in the host's DM (see Fig. 1). Massive satellites also induce a reflex motion of up to tens of kpc in the position of the host's inner halo within its outer halo, which alters the orbits of other satellites and halo tracers (e.g. Erkal+2019, Garavito-Camargo+2021b, Vasiliev+2021,2022). M33 and M31 have a similar mass ratio (~10%) as the LMC and MW (G19, P17, and references therein), so it is expected that M33 has a comparably large influence on M31's halo and on the orbits of its other satellites. M33's effects on M31 are asymmetric, time-dependent, and cannot be captured by simple models such as those currently in use. *If the perturbations induced by M33 remain unaccounted for, the orbits of M31 satellites—including that of M33 itself—cannot be confidently derived.*

As the number of M31 satellites with measured PMs grows, there is an urgent need for a theoretical framework with which to interpret the 3-D velocities of the satellites. Current models specifically lack a description of how the M31 and M33 halos *change shape* in response to each other as a function of time. High-resolution *N*-body simulations, such as those proposed here, remain the only viable way to fully model the interaction of two DM halos, including the effects of the satellite on its host as well as the effect of the host's tides on the satellite.

3. Mapping M33's Influence on M31's Dark Matter Distribution Requires *N*-body Simulations

<u>We propose to use state-of-the-art high-resolution (m~$10^4\ M_\odot$, N~2.2×10^8) *N*-body simulations of the M31/M33 interaction to fully capture how M31 and M33's halos are distorted in response to each other.</u> Our simulation suite will include both the first-infall orbit (P17) and recent pericenter passage orbit (McConnachie+2009, Putman+2009) scenarios (see Fig. 2), while also varying the masses of M31 and M33 as well as the velocity anisotropy profile of M31's halo. In all cases, our simulations will be designed to reproduce the current locations of M31 and M33 in 6-D phase space, as measured by *HST* (GO-11684, PI Sohn) and other facilities. Importantly, such *N*-body simulations are required to fully model the halos' responses to each other. While complementary analytic methods such as linear response theory can describe the satellite's effects on the host, they do not yet capture the effects of the host's tides on the satellite (Rozier+2022).

Previous work on the MW/LMC system has both proven the effectiveness of the techniques proposed here and highlighted the need for new models tailored specifically to the M31/M33 system (G19, Garavito-Camargo+2021a,b). In particular, the perturbations induced in the host's halo by a massive satellite depend on the satellite's orbit: the transient response (dynamical friction wake; Chandrasekhar 1943) traces the satellite's orbital path, while the collective response arises from the reflex motion of the host's inner halo about the system's barycenter. Analytic work by Rozier+(2022) also shows the dependence of the perturbations on the satellite's orbit. Thus, the novel models proposed here are necessary to describe the combined M31+M33 DM distribution, accounting for both of M33's possible orbital histories.

4. Rapid Orbit Integration of M31 Satellites Using Analytic Potentials

To quantify the structure and gravitational potential of the M31/M33 DM distribution in our simulations, we will use a BFE technique (Hernquist & Ostriker 1992) to extract an analytic description of the combined halo (see Fig. 3). Specifically, we expand the density field and potential from each simulation snapshot in a series of orthogonal basis functions, using the publicly available `Gala` code (Price-Whelan 2017) as modified by Garavito-Camargo+(2021a) for use with simulations of this type. The code outputs the values of the expansion terms' coefficients for each snapshot. When interpolated, the result is a set of functions in time that describe the coefficients' evolution during the simulations, providing a fully analytic description of the M31/M33 DM density field and gravitational potential.

For each simulation in our suite, we will publish the time-dependent BFE coefficients, and also place the BFE potentials into `Gala`, making our cutting-edge models widely accessible to the community. These data products will allow fast and accurate orbit integration of M31 satellites and other halo tracers as their PMs become available, without the need to run additional expensive *N*-body simulations.

The proposed program will widely disseminate the necessary foundation to interpret 6-D phase space information afforded by *HST*, greatly enhancing the legacy value of both existing and future datasets. For example, revisiting PM measurements of the GPoA (GO-16273, PI Sohn) and M31 (GO-11684, PI Sohn) with our models will shed light on the existence of and causes for the plane, similar to an analysis of the MW's satellite plane by Garavito-Camargo+(2021a). Additionally, ongoing *HST* first-epoch observations (GO-15902, PI Weisz) and planned *JWST* second-epoch observations will provide PM measurements of the entire system. When combined with our models, these datasets will produce the most comprehensive understanding of M31 satellite orbits to date.

5. A Complete Picture of the Dynamics of the Local Group and New Probes of Dark Matter Physics

Reconstructing the orbits of M31 satellites using the proposed BFE potentials will finally unveil the assembly history of the M31 system, opening the door for a wealth of future studies. For example, our work will provide a description of the dynamics of other satellites and halo tracers in both possible M33 orbit scenarios, which will allow observations to distinguish the two scenarios. M31's assembly history can also be compared to expectations from cosmological simulations to test theories of galaxy formation and evolution in the ΛCDM paradigm (e.g. Boylan-Kolchin+2011; P17, Patel+2018).

Understanding the dynamics of the M31 system will place the MW into context both within the Local Group and cosmologically. For instance, a comprehensive understanding of satellite orbits in the Local Group will help unravel the mysteries of the MW and M31's satellite planes (Ibata+2013, Pawlowski+2018) by potentially offering dynamical arguments for their existence (Garavito-Camargo+2021a). Additionally, Chamberlain+(2022) showed that timing argument measurements of the Local Group mass are affected by host reflex motions due to satellites. While they argue M31's reflex motion due to M33 is expected to be weaker than the MW's reflex motion due to the LMC, our work will provide the first estimates of the M31 reflex motion, allowing the Local Group mass to be more accurately constrained.

Observations of the distributions of halo tracers besides satellites, such as globular clusters, stellar streams, and halo stars, can be cross-checked with expectations based on the potentials derived from our simulations. For example, the dynamical friction wakes of massive satellites can be detected using stellar halo tracers (G19, Conroy+2021). Coupled with expectations that the morphology and density of dynamical friction wakes depend on the microphysics of the DM particle (e.g. Furlanetto & Loeb 2002, Lancaster+2020), our simulations will lay the CDM groundwork for studying M33's wake as a probe of DM physics. In short, our proposed models will allow the community to take advantage of the game-changing accuracy of *HST* PMs to push the frontier for studying galaxy assembly physics and the connection between galaxies and their DM.

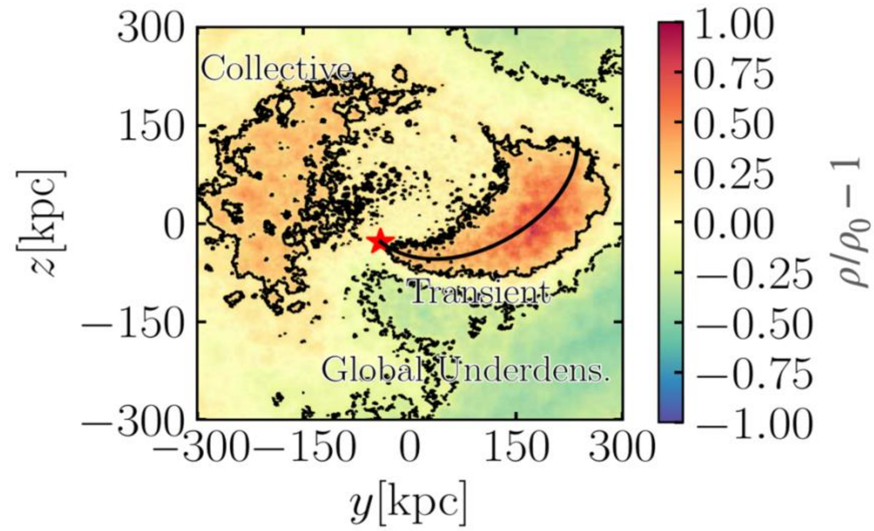

Fig 1. Perturbations induced in the MW's DM by the LMC from an *N*-body simulation by G19, illustrating the impacts of a massive satellite on its host. The colorbar denotes the density contrast in the MW's DM caused by the LMC, compared to an isolated MW halo. The LMC's location is shown by the star, and its orbit by the black line. Coordinates are centered on the MW disk. Massive satellites induce two overdensities in their host's DM: 1) a transient response (dynamical friction wake; Chandrasekhar 1943) trailing the satellite along its orbit and 2) a collective response leading the satellite, due to the reflex motion of the host's inner halo. The perturbations are highly asymmetric, time-dependent, and are sensitive to the satellite's orbit. *The proposed work will model these perturbations in the M33/M31 system for the first time.* Adapted from G19.

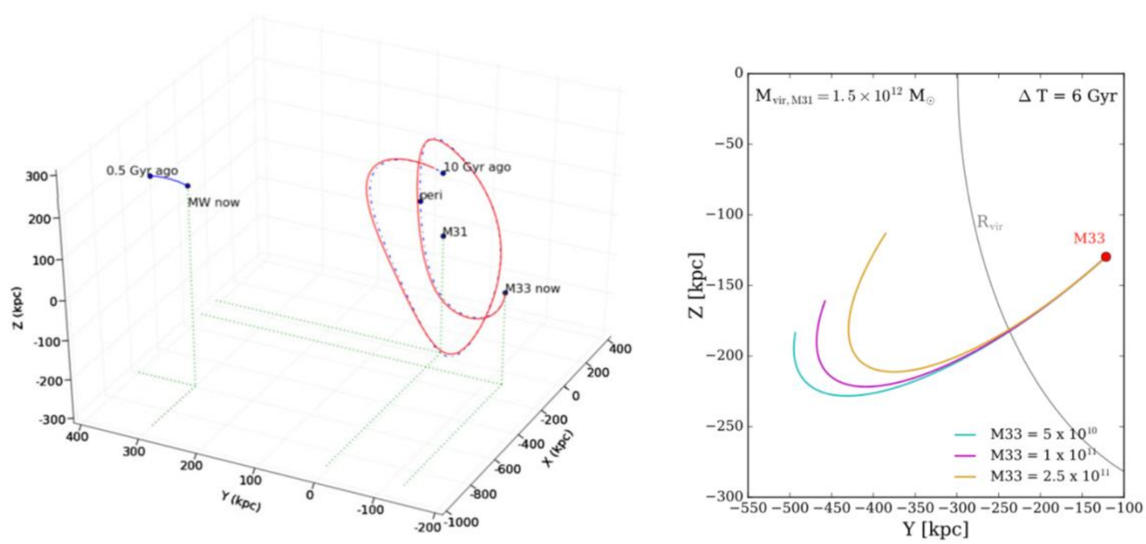

A) M33 completes multiple orbits

B) M33 on First Infall

Fig 2. Possible orbital histories of M33. M31's position is the coordinate origin in both panels. *Panel A*: Recent pericenter passage scenario. M33's orbit is integrated for 10 Gyr, and is shown by the solid red line when only considering M31's gravity, or by the blue dotted line when considering the MW's gravity as well. M33 experiences a pericenter passage 1.6 Gyr ago, reaching a minimum galactocentric distance of ~10 kpc. Adapted from Putman+(2009). *Panel B*: First-infall scenario. M31's virial radius is denoted by the grey circle. M33's orbit is integrated for 6 Gyr. Different lines show the effect of changing M33's mass. In all three cases, M31 is on its first infall to M31's halo. Adapted from P17. *The proposed simulation suite will include models of both orbital scenarios.*

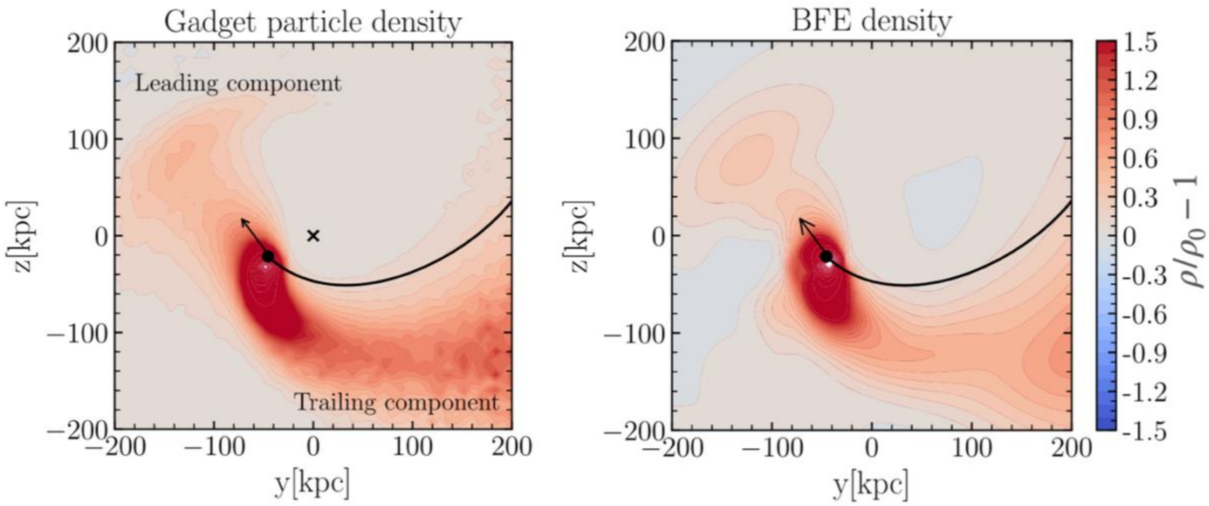

Fig 3. BFE reconstruction of the density field in an *N*-body simulation from the same LMC/MW suite as Fig. 1, highlighting the accuracy of the BFE technique. The colorbar shows the density contrast of the LMC's DM compared to the MW halo (compared to Fig. 1 which only includes MW particles). The position of the MW's cusp is shown by the x, while the LMC's cusp, orbit, and velocity vector are shown by the dot, line, and arrow, respectively. The left panel shows the particle density field from the simulation, while the right panel shows the BFE reconstruction. The BFE accurately captures the complex structure of the tidally disrupting LMC halo from the simulation. *We will apply this technique to our simulations to extract an analytic, time-dependent potential for the combined M31/M33 system, and release these potentials to the community.*

- **References**

Bonaca A., Geha M., Küpper A. H. W. *et al., 2*014, ApJ, 795, 94
Bonaca A. & Hogg D. W., 2018, ApJ, 887, 101
Bonaca A., Hogg D. W., Price-Whelan A. M., & Conroy C., 2019, ApJ, 880, 38
Boylan-Kolchin M., Besla G., & Hernquist L., 2011, MNRAS, 414, 1560
Brunthaler, A., Reid M. J., & Falcke H. *et al.*, 2005, Science, 307, 1440
Carlberg R. G., 2017, ApJ, 838, 39
Chamberlain K., Price-Whelan A. M., Besla G. *et al.*, 2022, arXiv preprint, arXiv:2204.07173
Chandrasekhar, S., 1943, ApJ, 97, 255
Conroy C., Naidu R. P., Garavito-Camargo N. *et al.*, 2021, Nature, 593, 534
Erkal D., Belokurov V., Laporte C. F. P. *et al.*, 2019, MNRAS, 487, 2685
Furlanetto S. R. & Loeb A., 2002, ApJ, 565, 854
Garavito-Camargo N., Besla, G., Laporte, C. F. P. *et al.*, 2019, ApJ, 884, 51
Garavito-Camargo N., Patel E., Besla G. *et al.*, 2021, ApJ, 923, 140
Garavito-Camargo N., Besla G., Chervin C. F. P. *et al.*, 2021, ApJ, 919, 109
Gómez F. A., Besla G., Carpintero D. D. *et al.*, 2015, ApJ, 802, 128
Hernquist L. & Ostriker J. P., 1992, ApJ, 386, 375
Ibata R. A., Lewis G. F., Conn A. R. *et al.*, 2013, Nature, 493, 62
Kruijssen J. M. D., Pfeffer J. L., Reina-Campos M. *et al.*, 2019, MNRAS, 486, 3180
Lancaster L., Giovanetti C., Mocz P. *et al.*, 2020, JCAP, 01, 001
McConnachie A. W., Irwin M. J., Ibata R. A. *et al.*, Nature, 461, 66
Naidu R. P., Conroy C., Bonaca A. *et al.*, 2021, ApJ, 923, 92
Patel E., Besla G., & Sohn S. T., 2017, MNRAS, 464, 3825

Patel E., Besla G., & Mandel K., 2017, MNRAS, 468, 3428
Patel E., Carlin J. L., Tollerud E. J. *et al.*, 2018, MNRAS, 480, 1883
Patel E., Kallivayalil N., Garavito-Camargo N. *et al.*, 2020, ApJ, 893, 121
Pawlowski M. S., 2018, MPLA, 33, 1830004
Pawlowski M. S., Pflamm-Altenburg J., & Kroupa P., 2012, MNRAS, 423, 1109
Price-Whelan A. M., 2017, JOSS, 2(18), 388
Price-Whelan A. M., Hogg D. W., Johnston K. V., & Hendel D., 2014, ApJ, 794, 4
Putman M. E., Peek J. E. G., Muratov A. *et al.*, 2009, ApJ, 703, 1486
Rozier S., Famaey B., Seibert A. *et al.*, 2022, arXiv preprint, arXiv:2201.05589
Sohn S. T., Anderson J., & van der Marel, R. P., 2012, ApJ, 753, 7S
Sohn S. T., Patel E., Fardal, M. A. *et al.*, 2020, ApJ, 901, 43
van der Marel, R. P., Fardal, M. A., Sohn S. T. *et al.*, 2019, ApJ, 872, 24
Vasiliev E., Belokurov V., & Erkal D., 2021, MNRAS, 501, 2279
Vasiliev E., Belokurov V., & Evans, N. W., 2022, ApJ, 926, 203